Nanostructured Mg-Based Hydrogen Storage Systems

Subjects: Materials Science, Characterization & Testing

Contributor: Ádám Révész

As the most abundant element in the world, hydrogen is a promising energy carrier and has received continuously growing attention in the last couple of decades. At the very moment, hydrogen fuel is imagined as the part of a sustainable and eco-friendly energy system, the “hydrogen grand challenge”. Among the large number of storage solutions, solid-state hydrogen storage is considered to be the safest and most efficient route for on-board applications via fuel cell devices. Notwithstanding the various advantages, storing hydrogen in a lightweight and compact form still presents a barrier towards the wide-spread commercialization of hydrogen technology. In this review paper we summarize the latest findings on solid-state storage solutions of different non-equilibrium systems which have been synthesized by mechanical routes based on severe plastic deformation. Among these deformation techniques, high-pressure torsion is proved to be a proficient method due to the extremely high applied shear strain that develops in bulk nanocrystalline and amorphous materials.

high-pressure torsion severe plastic deformation hydrogen storage Mg-based alloys

1. Elemental Mg and MgH_2

As was described in the Introduction part of this Review, solid-state hydrogen storage is still a significant technological challenge, nevertheless, numerous promising efforts have been occurred so far. Among metallic elements, magnesium attracts the highest interest in the field of solid-state hydrogen storage due to its very high theoretical gravimetric capacity (7.6 wt.%). It was found that at temperatures and hydrogen partial pressures of practical interest of H-storage, the α-MgH_2 tetragonal rutile structure is stable and stoichiometric (see Figure 1), in accordance with the small H-vacancy concentration [1].

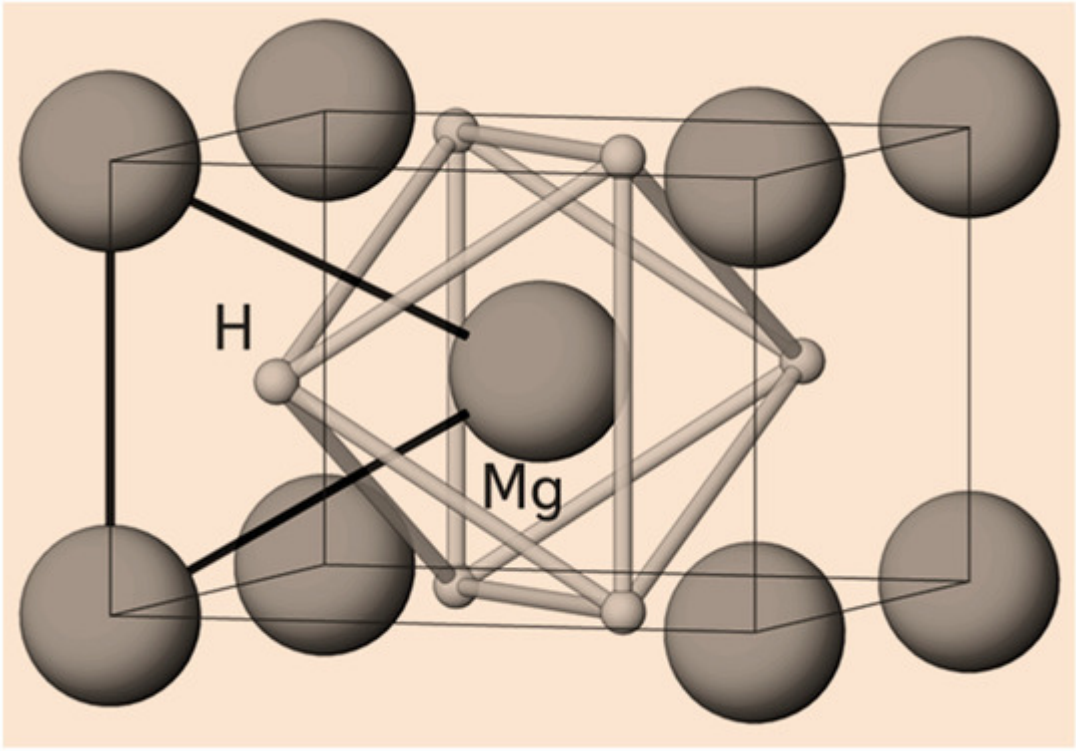

Figure 1. Tetragonal crystalline lattice of the rutile-type α-MgH_2 phase.

Magnesium has several other advantages, i.e., it is lightweight, non-toxic, abundant and cheap [2][3][4]. On the other hand, the very high formation enthalpy (ΔH = −78 kJ/mol) of the MgH_2 phase (i.e., the high strength of the Mg–H bonds), the high activation energy of H_2 dissociation, and the sluggish sorption kinetics are the major drawbacks of on-board commercialization of MgH_2 [3]. In order to overcome these difficulties, it is important to develop the kinetic and thermodynamic performance of Mg-based systems simultaneously. Until now, a large number of attempts have been targeted to deal with these issues, including nanostructuring by HEBM [5][6][7], which can significantly enhance the hydrogenation kinetics, particularly the diffusion of hydrogen due to the abundant grain boundaries and lattice defects [8][9][10]. Due to the different coordination number of the Mg and H atoms in the grain boundary region, the surface morphology usually can affect both the kinetic and thermodynamic performance of the Mg-nanoparticles [11]. The advantage of HEBM is not only manifested in rapid crystallite-size decrease, but the generation of metastable orthorhombic γ-MgH_2 phase results in the decrease of the hydrogen sorption temperature [12].

The microstructural characterization of consolidated MgH_2 powders revealed that significant grain refinement of the hydride phase takes place during the HPT deformation with the average crystallite size in the range of 20 nm [13]. The severe shear deformation also provokes a strong (002) texture and the formation of the metastable *y*-MgH_2 phase. When HPT is applied for a different number of whole revolutions under p = 6 GPa to deform compacted α-MgH_2 micropowders, the material starts to transform into nanocrystalline high-pressure *y* phase [14]. As presented by the TEM micrographs in Figure 2, the shear strain leads to a significant crystallite size reduction after *N* = 15 whole turns (~70 nm), while the selected area diffraction (SAED) patterns and the corresponding fast Fourier transform (FFT) diffractograms confirm the gradual formation of the high pressure phase. This phase

exhibits a lower hydrogen binding energy and accordingly a lower dehydrogenation temperature (T~610 K). This study pointed out that varying the crystal structure is an efficient approach to destabilize the hydrides without compositional changes [14]. In a recent comparative research, H-sorption behavior was analyzed on two different types of HPT consolidated Mg powder precursors. The results showed that the nature of the initial powders has a pronounced effect, i.e., the compacts prepared from ultrafine powder obeys faster absorption kinetics than the consolidated product obtained from micro-sized atomized powder [15]. Nevertheless, the latter sample can absorb more hydrogen and exhibits enhanced desorption.

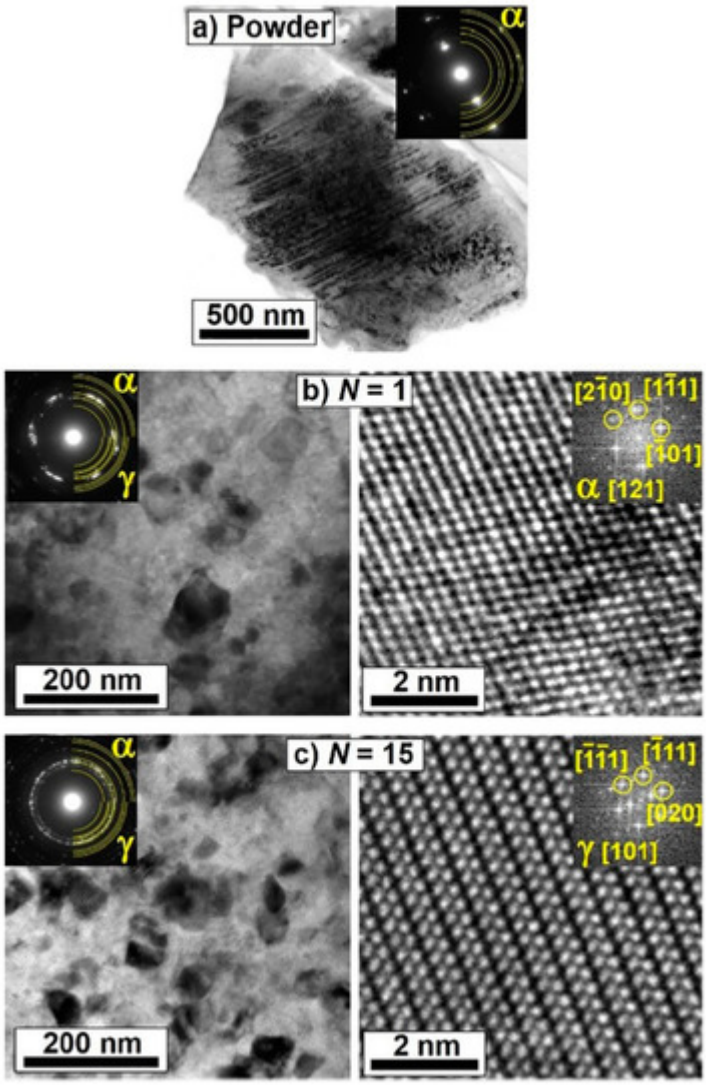

Figure 2. TEM images and corresponding SAED patterns (left) together with high-resolution lattice images and corresponding FFT diffractograms (right) for (**a**) tetragonal α-MgH_2 powder, disk processed by HPT under p = 6 GPa for (**b**) *N* = 1 and (**c**) *N* = 15 whole turns [14].

When pure bulk Mg is torqued by HPT, a bimodal microstructure develops, including nanocrystals and large recrystallized grains with an average grain size of ~1 μm. After *N* = 10 torsion numbers, the hydrogenation improves significantly and the absorption rate is increased [16]. This phenomenon is mainly attributed to the presence of high-angle grain boundaries. The average dislocation density obtained from X-ray line profile analysis

of commercial Mg disks processed by HPT reaches a very large value ($\rho = 8 \cdot 10^{15}$ m^{-2}) at $N = 10$, referring to the extreme intensity of shear deformation. The hydrogen storage capacity increases with increasing N due to the formation of dislocations, which can act as hydrogen absorption sites [17]. The hydrogen storage capacity was found to be stable up to 200 hydrogenation/dehydrogenation cycles for the ZK60 Mg-alloy (Mg-5.8Zn-0.57Zr, element concentration in wt.%) processed by HPT [18]. At the same time, both the absorption and desorption curves can satisfactorily be fitted by the Johnson-Mehl-Avrami function with an exponent n = 1 for all investigated cycling numbers (see Figure 3), which can be attributed to the high density of hydride nuclei hindering each other to grow.

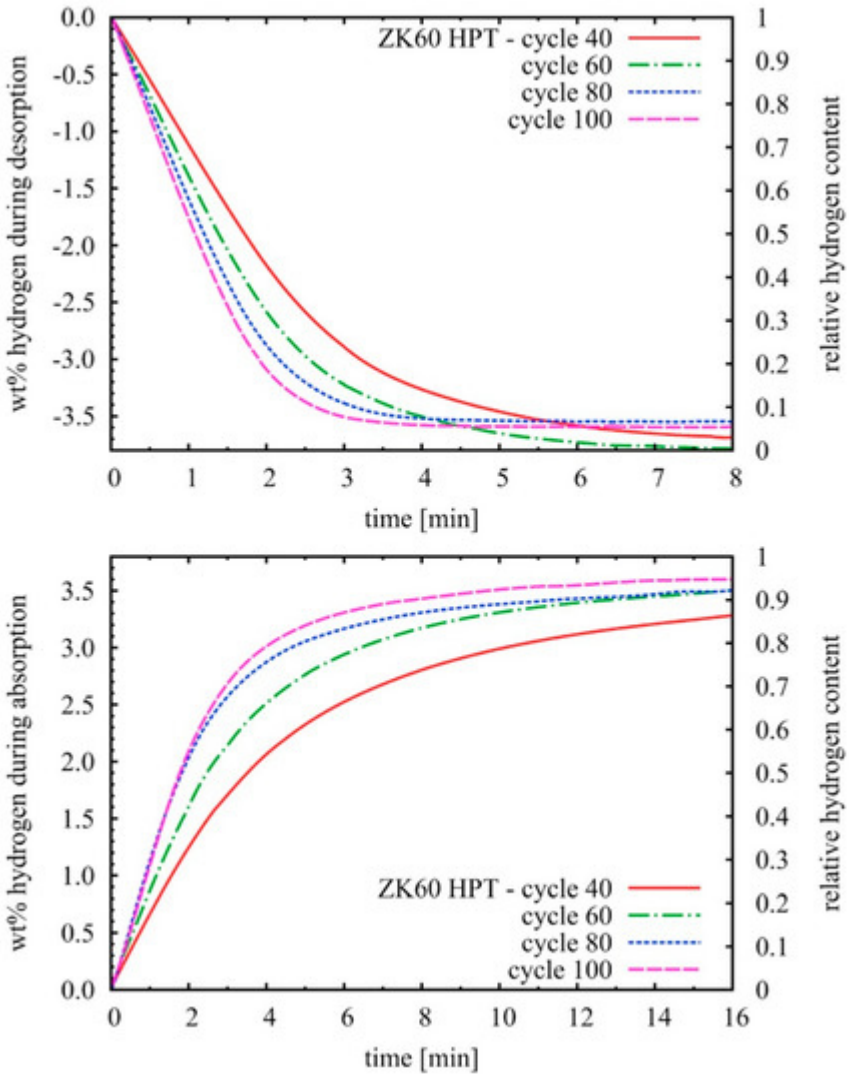

Figure 3. Dehydrogenation (**top**) and hydrogenation kinetic curves (**bottom**) obtained at 350 °C, 10 bar absorption pressure, 0.001 bar desorption pressure of the HPT-deformed ZK60 alloy [18].

2. Mg-Ni System

Alloying Ni to Mg by HEBM results in an excellent combination of advantageous thermodynamics [19] and improved hydrogen sorption by accelerating the recombination/dissociation of hydrogen atoms at the grain boundaries [20][21]. Based on the binary Mg-Ni phase diagram, the two elements are mutually insoluble [22], while two intermetallic line

compounds, i.e., Mg_2Ni and $MgNi_2$ exist, nonetheless only Mg_2Ni reacts with hydrogen with a 3.62 wt.% gravimetric capacity [23]. Moreover, a remarkable reduction of hydrogen desorption temperature was obtained when MgH_2 was catalyzed by Ni [24][25]. By varying HEBM parameters and the composition of the Mg-Ni powder blend, either a Mg + Ni → Mg_2Ni mechanochemical reaction [26][27][28] or (partial) solid state amorphization can take place [29].

In pioneering research carried out on the HPT deformation of the Mg-Ni system, it was demonstrated that the extreme shear deformation can reach such levels that it is capable to provoke hydrogen absorption in the otherwise non-absorbing $MgNi_2$ phase [30]. In recent work, it was demonstrated that the maximum H-absorption capacity of a $Mg_{70}Ni_{30}$ alloy is increased by 30–50% after HPT with respect to HEBM and can reach the theoretical value, due to the creation of new possible hydrogen absorption sites at the grain boundaries and near the vicinity of dislocations generated during the simultaneous compression and torsional straining [31]. Besides dislocations, other lattice defects, like stacking faults clearly improve the kinetics of Mg_2Ni processed by HPT [32]. It was also suggested that a large fraction of cracks can act as pathways to transport the hydrogen from the surface of the HPT disk and activate the material with fast kinetics. A new processing route, i.e., HPT of ultrafine Mg + 2wt.% Ni powder prepared by arc plasma evaporation significantly improves the H-kinetics and results in a hydrogen uptake at 100 °C [33]. Interestingly, the co-deformation of 2 wt.% Fe to Mg by HPT has a negligible effect on the H-storage performance of Mg, probably because ultrafine Fe powder particles did not intermix with Mg.

Partially hydrogenated and dehydrogenated states of a nanocrystalline $Mg_{75}Ni_{25}$ sample processed by HEBM and subsequent HPT technique revealed the formation of $Mg_2NiH_{0.3}$ hexagonal solid solution and the monoclinic Mg_2NiH_4 hydride phase during absorption [34]. The desorption induced changes in the relative amount of the two hydride phases indicated that the volumetric decrease of Mg_2NiH_4 and $Mg_2NiH_{0.3}$ is not simultaneous, i.e., at the initial stage of dehydrogenation, the decomposition of Mg_2NiH_4 is favored, while subsequently, the $Mg_2NiH_{0.3}$ → $Mg_2Ni + 0.3H_2$ reaction becomes more dominant (see Figure 4). It was also shown that the combination of HEBM and HPT is an effective deformation route to preserve the nanostructure of the alloy during the entire hydrogenation-dehydrogenation process. Complimentary high-pressure calorimetry confirmed a two-step sorption sequence both upon heating and cooling [35]. At the early stage of decomposition, the desorption of Mg_2NiH_4 occurs which is followed by the dehydrogenation of $Mg_2NiH_{0.3}$ solid solution. The enthalpy of hydrogenation/dehydrogenation reactions determined from the corresponding van't Hoff plots suggests that HPT promotes the destabilization of the metal-hydrogen bonds.

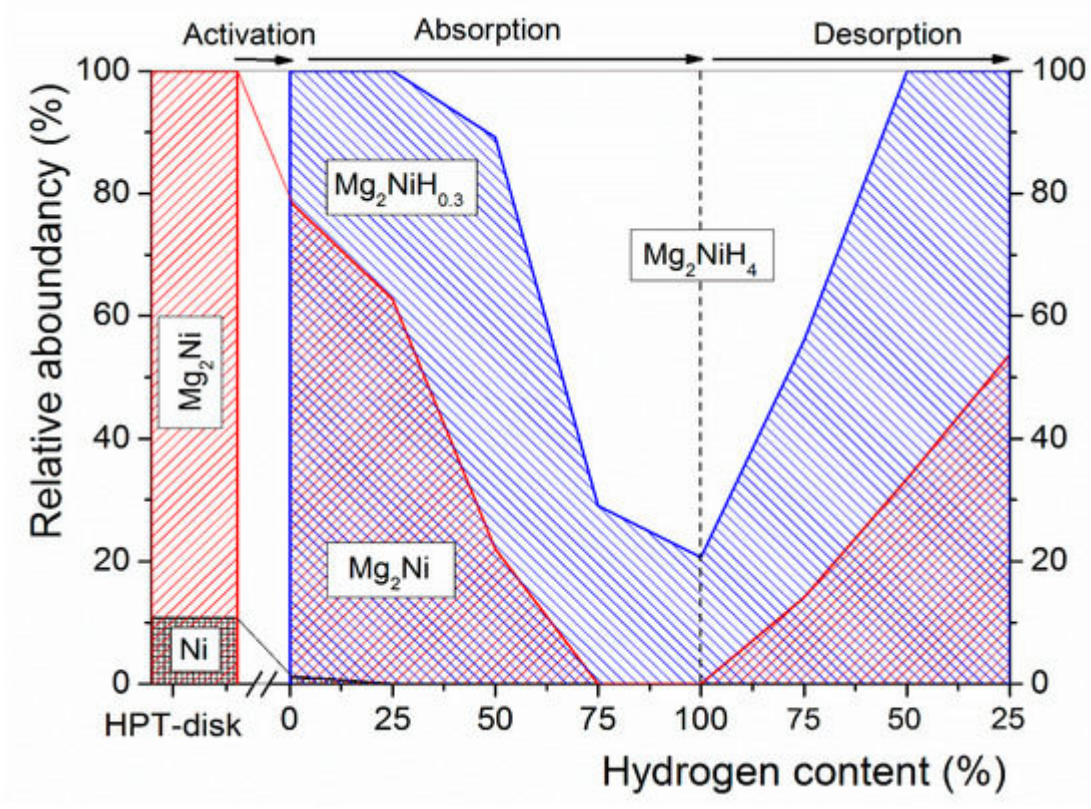

Figure 4. Evolution of phase composition during hydrogenation and dehydrogenation of the Mg-Ni HPT-disk [34].

3. Formation of New Hydrogen Storage Phases by HPT in Other Mg-Based Systems

The large plastic strain accompanying the high-pressure torsion procedure not only results in the reduction of the grain size and introduction of lattice defects but also new stable and even metastable phases can form in certain systems [36]. Accordingly, Mg_2Sn and Mg_2Ni intermetallics have formed after N = 100 rotations in Mg-V-Sn and Mg-V-Ni systems, respectively. Further increasing the number of revolutions results in the evolution of metastable phases in the Mg-V-Pd [36] alloy. It is noted that the corresponding binary systems have negative (Mg-Pd [37] and Pd-V) and positive mixing enthalpies (Mg-V [36]) as well. It was also revealed that metastable phases can develop even in immiscible systems with positive heat of mixing such as Mg-Ti [38] and Mg-Zr [39].The ultra-severe plastic deformation can extend the solubility of the minor components, thus new hydrogen storing materials can be manufactured. For example, in the Mg-Zr system N = 1000 revolutions results in significant mixing of Mg and Zr (see Figure 5). Mutual dissolution of elements in the Mg-Ti [39] and Mg-Zr [37] systems were observed by scanning electron microscopy, whilst the formation of BCC, FCC and HCP Mg-Ti [39] and HCP Mg-Zr phases [37] were confirmed by X-ray diffraction. Furthermore, during shear straining of MgH_2-TiH_2 mixture metastable ternary Mg-Ti-H hydride phase develops [40].

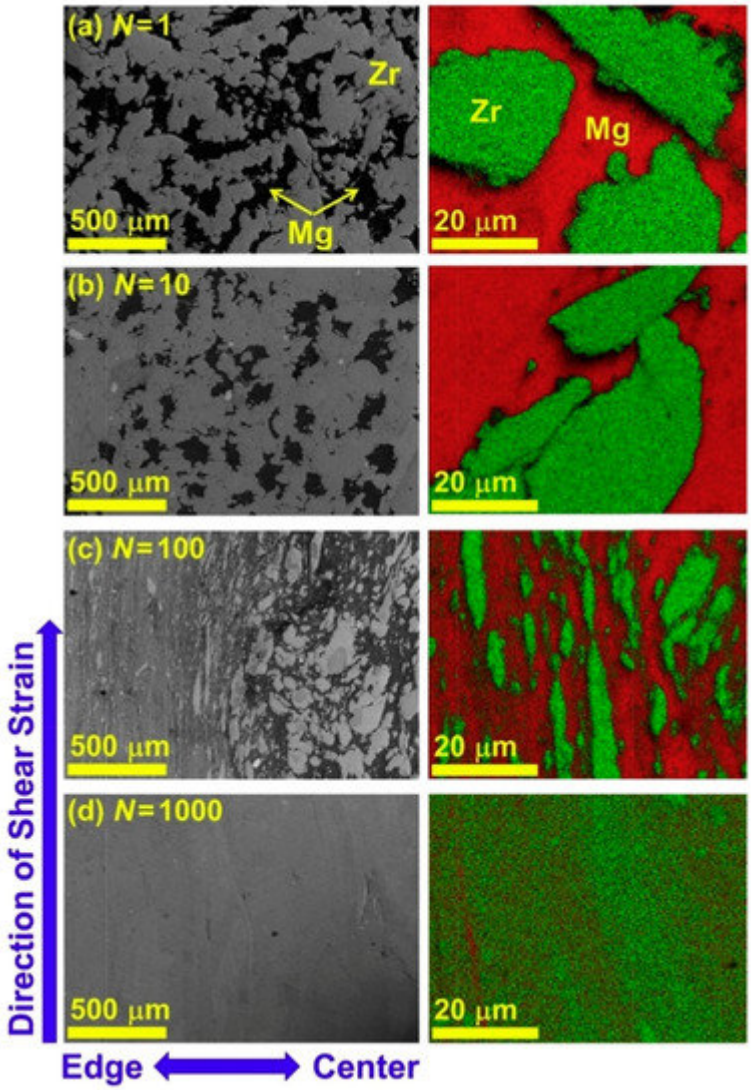

Figure 5. Scanning electron micrographs and EDS elemental mappings of the Mg-Zr alloy processed by HPT for different number of revolutions [39].

A first principle calculation to design Mg-based alloys with low binding energy was recently reported [41]. Accordingly, a Mg_4NiPd alloy of CsCl-type BCC structure has been fabricated by HPT through N = 1500 revolutions. This alloy is highly metastable, preserves its structure up to 440 K and possesses an extremely low (close to zero) hydrogen binding energy which enables reversible absorption and desorption of hydrogen at room temperature. At the same time, the reversible storage performance remains stable after five sorption cycles. This pioneering work of Edalati et al. demonstrated first that tuning the dehydrogenation temperature of Mg-based alloys to room temperature is possible by applying binding energy principles. As a continuation of this concept, a metastable FCC structure was also generated by HPT in the Mg-Hf binary system, however, attempts to produce magnesium-hafnium hydrides have been unsuccessful so far [42].

A recent paper has demonstrated that high-pressure torsion can be utilized for the synthesis of high-entropy materials for hydrogen storage [43]. MgVCr BCC and MgVTiCrFe high-entropy alloys were successfully synthesized via the combination of HEBM and HPT. The structure of the MgVTiCrFe product exhibits nanocrystalline and

amorphous character. Nevertheless, it was shown that the MgVCr possesses higher hydrogen storage capacity, better kinetics and phase stability compared to the MgVTiCrFe alloy.

4. Nanocrystalline Mg Catalyzed by Nanotube Additives

Several recent researches have been dedicated to the addition of carbon nanotubes (CNT) to nanocrystalline hydrogen storage materials to improve the kinetic behavior during absorption and desorption. It was demonstrated that only a few wt.% of CNT results in greatly enhanced kinetics of sorption reactions in Mg-Ni alloys [44][45]. CNT catalyzed Mg was able to absorb approximately 1.5 times more hydrogen than its uncatalyzed counterpart during the first couple of minutes of hydrogenation [46]. Based on these works, it is believed that the role of the carbon nanotubes in absorption/desorption reactions is to provide fast diffusion channels for the hydrogen atoms through a surface passivation layer into the bulk material [44][47]. Apart from the kinetic improvements, it was also proved that CNT addition is an efficient way to improve the long-term cycling stability of MgH_2 [48][49]. It was indicated that a synergetic effect may emerge between CNTs and other types of catalysts, such as Co [50], TiF_3 [48], or Nb_2O_5 [51].

In a recent research, the influence of the different deformation routes on the microstructural evolution and hydrogen storage behavior of nanocrystalline Mg catalyzed by Nb_2O_5 and/or CNT have been demonstrated [52]. The systematic kinetic analysis of the hydrogen sorption of Mg catalyzed by these additives is presented in Figure 6 [52]. As seen, the addition of Nb_2O_5 is important to achieve appropriate hydrogen sorption properties, however, it is also evident that the combination of the HEBM+HPT process or the addition of CNT catalyst can further improve the desorption kinetics of nanocrystalline Mg. The observed improvement was appropriated to the (002) texture (which is preserved during cycling) developed through the HPT procedure. Post-cycling XRD experiments demonstrated that the HPT processing or the CNT additive prevents excessive grain growth during cycling. A high resolution TEM image of the Mg-NbO-CNT disks confirms that the main portion of the CNTs is preserved during the extreme plastic deformation of HEBM, subsequent HPT, and hydrogenation/dehydrogenation cycling (see Figure 6) [52]. It was also shown that HEBM parameters also significantly affect the sorption performance of the final Mg-NbO-CNT HPT samples [53].

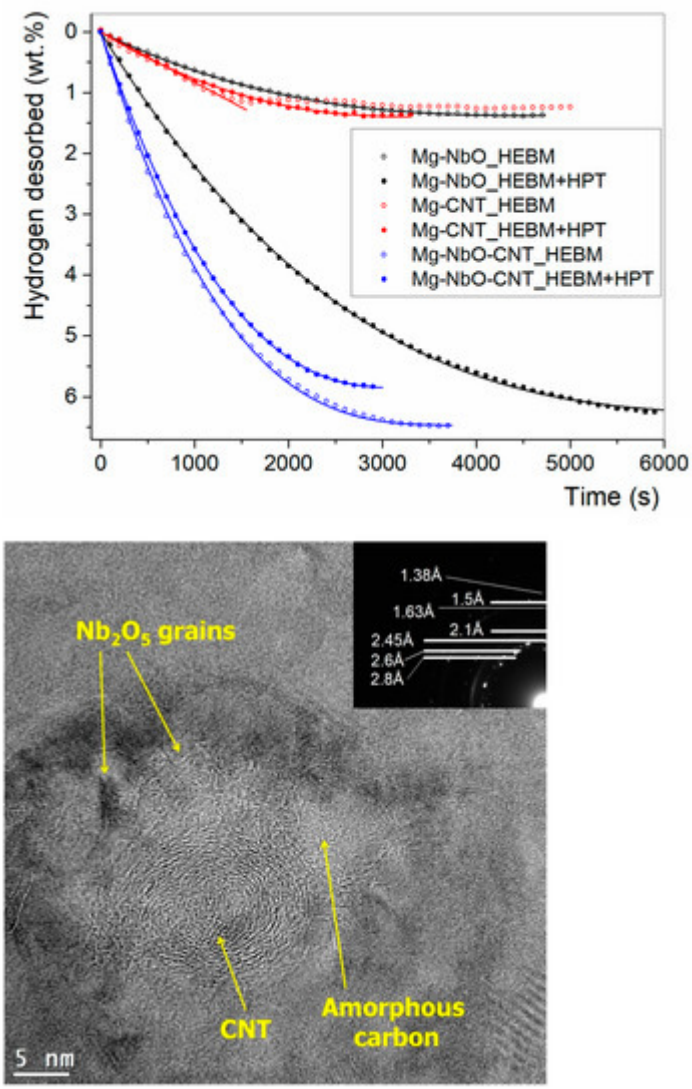

Figure 6. Measured desorption kinetic curves obtained at 573 K and p = 1 kPa of the as-milled powder samples and HPT-disks, with fitted model functions (**top**). HR-TEM image of the cycled Mg-NbO-CNT_HPT disk, the inset shows a typical SAED pattern (**bottom**) [52].

In a very recent paper, we have shown that the combined catalytic effect of metal-oxide particles and CNTs can be replaced by applying only titanate nanotubes (TN) [54], note that this research is still in progress. In this preliminary work, the HEBM+HPT deformation route was applied on nanocrystalline Mg powders catalyzed by TN. As was shown the HPT processing results in the decrease of the average crystallite size of HEBM Mg powders and at the same time a strong texture was also developed. In addition, the processing route considerably influences the H-sorption kinetics, i.e., the hydrogenation performance (capacity and kinetics) of the composite produced for longer co-milling of TN together with Mg significantly exceeds the sorption properties of the specimen when Mg was pre-milled and then milled together with TN for a short time. This observation can be attributed to the different morphology of the additives (better dispersed and partially damaged TN sections) and less to the microstructural parameters of the nanocrystalline Mg phase.

References

1. Grau-Crespo, R.; Smith, K.C.; Fisher, T.S.; de Leeuw, N.H.; Waghmare, U.V. Thermodynamics of Hydrogen Vacancies in MgH2 from First-Principles Calculations and Grand-Canonical Statistical Mechanics. Phys. Rev. B 2009, 80, 174117.
2. Schlapbach, L.; Züttel, A. Hydrogen-Storage Materials for Mobile Applications. Nature 2001, 414, 353–358.
3. Varin, R.A.; Czujko, T.; Wronski, Z.S. Nanomaterials for Solid State Hydrogen Storage; Springer Science: New York, NY, USA, 2009.
4. Züttel, A. Materials for Hydrogen Storage. Mater. Today 2003, 6, 24–33.
5. Zaluski, L.; Zaluska, A.; Tessier, P.; Stroem-Olsen, J.O.; Schulz, R. Nanocrystalline Hydrogen Absorbing Alloys. Mater. Sci. Forum 1996, 225–227, 853–858.
6. Oelerich, W.; Klassen, T.; Bormann, R. Metal Oxides as Catalysts for Improved Hydrogen Sorption in Nanocrystalline Mg-Based Materials. J. Alloys Compd. 2001, 315, 237–242.
7. Fátay, D.; Révész, Á.; Spassov, T. Particle Size and Catalytic Effect on the Dehydriding of MgH2. J. Alloys Compd. 2005, 399, 237–241.
8. Crivello, J.-C.; Dam, B.; Denys, R.V.; Dornheim, M.; Grant, D.M.; Huot, J.; Jensen, T.R.; de Jongh, P.; Latroche, M.; Milanese, C.; et al. Review of Magnesium Hydride-Based Materials: Development and Optimisation. Appl. Phys. A 2016, 122, 97.
9. Fátay, D.; Spassov, T.; Delchev, P.; Ribárik, G.; Révész, A. Microstructural Development in Nanocrystalline MgH2 during H-Absorption/Desorption Cycling. Int. J. Hydrogen Energy 2007, 32, 2914–2919.
10. Révész, Á.; Fátay, D. Microstructural Evolution of Ball-Milled MgH2 during a Complete Dehydrogenation–Hydrogenation Cycle. J. Power Sources 2010, 195, 6997–7002.
11. Paidar, V. Magnesium Hydrides and Their Phase Transitions. Int. J. Hydrogen Energy 2016, 41, 9769–9773.
12. Zhou, S.; Zhang, Q.; Chen, H.; Zang, X.; Zhou, X.; Wang, R.; Jiang, X.; Yang, B.; Jiang, R. Crystalline Structure, Energy Calculation and Dehydriding Thermodynamics of Magnesium Hydride from Reactive Milling. Int. J. Hydrogen Energy 2015, 40, 11484–11490.
13. Leiva, D.R.; Jorge, A.M.; Ishikawa, T.T.; Huot, J.; Fruchart, D.; Miraglia, S.; Kiminami, C.S.; Botta, W.J. Nanoscale Grain Refinement and H-Sorption Properties of MgH2 Processed by High-Pressure Torsion and Other Mechanical Routes. Adv. Eng. Mater. 2010, 12, 786–792.
14. Edalati, K.; Kitabayashi, K.; Ikeda, Y.; Matsuda, J.; Li, H.-W.; Tanaka, I.; Akiba, E.; Horita, Z. Bulk Nanocrystalline Gamma Magnesium Hydride with Low Dehydrogenation Temperature Stabilized

by Plastic Straining via High-Pressure Torsion. Scr. Mater. 2018, 157, 54–57.

15. Panda, S.; Fundenberger, J.-J.; Zhao, Y.; Zou, J.; Toth, L.S.; Grosdidier, T. Effect of Initial Powder Type on the Hydrogen Storage Properties of High-Pressure Torsion Consolidated Mg. Int. J. Hydrogen Energy 2017, 42, 22438–22448.
16. Edalati, K.; Yamamoto, A.; Horita, Z.; Ishihara, T. High-Pressure Torsion of Pure Magnesium: Evolution of Mechanical Properties, Microstructures and Hydrogen Storage Capacity with Equivalent Strain. Scr. Mater. 2011, 64, 880–883.
17. Révész, Á.; Gajdics, M. Correlation between Microstructure and Hydrogen Storage Properties of Nanocrystalline Magnesium Subjected to High-Pressure Torsion. Mater. Sci. Forum 2017, 885, 67–73.
18. Grill, A.; Horky, J.; Panigrahi, A.; Krexner, G.; Zehetbauer, M. Long-Term Hydrogen Storage in Mg and ZK60 after Severe Plastic Deformation. Int. J. Hydrogen Energy 2015, 40, 17144–17152.
19. Zeng, K.; Klassen, T.; Oelerich, W.; Bormann, R. Thermodynamic Analysis of the Hydriding Process of Mg–Ni Alloys. J. Alloys Compd. 1999, 283, 213–224.
20. Liang, G.; Boily, S.; Huot, J.; Van Neste, A.; Schulz, R. Mechanical Alloying and Hydrogen Absorption Properties of the Mg–Ni System. J. Alloys Compd. 1998, 267, 302–306.
21. Zaluska, A.; Zaluski, L.; Ström-Olsen, J.O. Structure, Catalysis and Atomic Reactions on the Nano-Scale: A Systematic Approach to Metal Hydrides for Hydrogen Storage. Appl. Phys. A 2001, 72, 157–165.
22. Massalski, T.B.; Murray, J.L.; Bennett, L.H.; Baker, H. Binary Alloy Phase Diagrams; American Society for Metals: Materials Park, OH, USA, 1986; ISBN 978-0-87170-261-6.
23. Reilly, J.J., Jr.; Wishwall, R.H., Jr. Reaction of Hydrogen with Alloys of Magnesium and Nickel and the Formation of Mg2NiH4. Inorg. Chem. 1968, 7, 2254–2256.
24. Simchi, H.; Kaflou, A.; Simchi, A. Synergetic Effect of Ni and Nb2O5 on Dehydrogenation Properties of Nanostructured MgH2 Synthesized by High-Energy Mechanical Alloying. Int. J. Hydrogen Energy 2009, 34, 7724–7730.
25. Xie, L.; Li, J.; Zhang, T.; Kou, H. Understanding the Dehydrogenation Process of MgH2 from the Recombination of Hydrogen Atoms. Int. J. Hydrogen Energy 2016, 41, 5716–5724.
26. Urretavizcaya, G.; García, G.; Serafini, D.; Meyer, G. Mg-Ni Alloys For Hydrogen Storage Obtained By Ball Milling. Lat. Am. Appl. Res. 2002, 32, 289–294.
27. Varin, R.A.; Czujko, T.; Mizera, J. Microstructural Evolution during Controlled Ball Milling of (Mg2Ni+MgNi2) Intermetallic Alloy. J. Alloys Compd. 2003, 350, 332–339.

28. Révész, Á.; Gajdics, M.; Spassov, T. Microstructural Evolution of Ball-Milled Mg–Ni Powder during Hydrogen Sorption. Int. J. Hydrogen Energy 2013, 38, 8342–8349.
29. Orimo, S.; Ikeda, K.; Fujii, H.; Fujikawa, Y.; Kitano, Y.; Yamamoto, K. Structural and Hydriding Properties of the Mg-Ni-H System with Nano- and/or Amorphous Structures. Acta Mater. 1997, 45, 2271–2278.
30. Kusadome, Y.; Ikeda, K.; Nakamori, Y.; Orimo, S.; Horita, Z. Hydrogen Storage Capability of MgNi2 Processed by High Pressure Torsion. Scr. Mater. 2007, 57, 751–753.
31. Révész, Á.; Kánya, Z.; Verebélyi, T.; Szabó, P.J.; Zhilyaev, A.P.; Spassov, T. The Effect of High-Pressure Torsion on the Microstructure and Hydrogen Absorption Kinetics of Ball-Milled Mg70Ni30. J. Alloys Compd. 2010, 504, 83–88.
32. Hongo, T.; Edalati, K.; Arita, M.; Matsuda, J.; Akiba, E.; Horita, Z. Significance of Grain Boundaries and Stacking Faults on Hydrogen Storage Properties of Mg2Ni Intermetallics Processed by High-Pressure Torsion. Acta Mater. 2015, 92, 46–54.
33. Grosdidier, T.; Fundenberger, J.J.; Zou, J.X.; Pan, Y.C.; Zeng, X.Q. Nanostructured Mg Based Hydrogen Storage Bulk Materials Prepared by High Pressure Torsion Consolidation of Arc Plasma Evaporated Ultrafine Powders. Int. J. Hydrogen Energy 2015, 40, 16985–16991.
34. Gajdics, M.; Calizzi, M.; Pasquini, L.; Schafler, E.; Révész, Á. Characterization of a Nanocrystalline Mg–Ni Alloy Processed by High-Pressure Torsion during Hydrogenation and Dehydrogenation. Int. J. Hydrogen Energy 2016, 41, 9803–9809.
35. Révész, Á.; Gajdics, M.; Schafler, E.; Calizzi, M.; Pasquini, L. Dehydrogenation-Hydrogenation Characteristics of Nanocrystalline Mg2Ni Powders Compacted by High-Pressure Torsion. J. Alloys Compd. 2017, 702, 84–91.
36. Edalati, K.; Uehiro, R.; Fujiwara, K.; Ikeda, Y.; Li, H.-W.; Sauvage, X.; Valiev, R.Z.; Akiba, E.; Tanaka, I.; Horita, Z. Ultra-Severe Plastic Deformation: Evolution of Microstructure, Phase Transformation and Hardness in Immiscible Magnesium-Based Systems. Mater. Sci. Eng. A 2017, 701, 158–166.
37. Dębski, A.; Terlicka, S.; Gąsior, W.; Gierlotka, W.; Pęska, M.; Polański, M. Thermodynamic Properties of Mg-Pd Liquid Alloys. J. Mol. Liq. 2020, 317, 114024.
38. Edalati, K.; Emami, H.; Staykov, A.; Smith, D.J.; Akiba, E.; Horita, Z. Formation of Metastable Phases in Magnesium–Titanium System by High-Pressure Torsion and Their Hydrogen Storage Performance. Acta Mater. 2015, 99, 150–156.
39. Edalati, K.; Emami, H.; Ikeda, Y.; Iwaoka, H.; Tanaka, I.; Akiba, E.; Horita, Z. New Nanostructured Phases with Reversible Hydrogen Storage Capability in Immiscible Magnesium–Zirconium System Produced by High-Pressure Torsion. Acta Mater. 2016, 108, 293–303.

40. Kitabayashi, K.; Edalati, K.; Li, H.; Akiba, E.; Horita, Z. Phase Transformations in MgH2–TiH2 Hydrogen Storage System by High-Pressure Torsion Process. Adv. Eng. Mater. 2020, 22, 1900027.
41. Edalati, K.; Uehiro, R.; Ikeda, Y.; Li, H.-W.; Emami, H.; Filinchuk, Y.; Arita, M.; Sauvage, X.; Tanaka, I.; Akiba, E.; et al. Design and Synthesis of a Magnesium Alloy for Room Temperature Hydrogen Storage. Acta Mater. 2018, 149, 88–96.
42. López Gómez, E.I.; Edalati, K.; Coimbrão, D.D.; Antiqueira, F.J.; Zepon, G.; Cubero-Sesin, J.M.; Botta, W.J. FCC Phase Formation in Immiscible Mg–Hf (Magnesium–Hafnium) System by High-Pressure Torsion. AIP Adv. 2020, 10, 055222.
43. De Marco, M.O.; Li, Y.; Li, H.-W.; Edalati, K.; Floriano, R. Mechanical Synthesis and Hydrogen Storage Characterization of MgVCr and MgVTiCrFe High-Entropy Alloy. Adv. Eng. Mater. 2020, 22, 1901079.
44. Aminorroaya, S.; Liu, H.K.; Cho, Y.; Dahle, A. Microstructure and Activation Characteristics of Mg–Ni Alloy Modified by Multi-Walled Carbon Nanotubes. Int. J. Hydrogen Energy 2010, 35, 4144–4153.
45. Hou, X.; Hu, R.; Zhang, T.; Kou, H.; Li, J. Hydrogenation Thermodynamics of Melt-Spun Magnesium Rich Mg–Ni Nanocrystalline Alloys with the Addition of Multiwalled Carbon Nanotubes and TiF3. J. Power Sources 2016, 306, 437–447.
46. Chen, B.-H.; Kuo, C.-H.; Ku, J.-R.; Yan, P.-S.; Huang, C.-J.; Jeng, M.-S.; Tsau, F.-H. Highly Improved with Hydrogen Storage Capacity and Fast Kinetics in Mg-Based Nanocomposites by CNTs. J. Alloys Compd. 2013, 568, 78–83.
47. Su, W.; Zhu, Y.; Zhang, J.; Liu, Y.; Yang, Y.; Mao, Q.; Li, L. Effect of Multi-Wall Carbon Nanotubes Supported Nano-Nickel and TiF3 Addition on Hydrogen Storage Properties of Magnesium Hydride. J. Alloys Compd. 2016, 669, 8–18.
48. Shahi, R.R.; Bhatnagar, A.; Pandey, S.K.; Dixit, V.; Srivastava, O.N. Effects of Ti-Based Catalysts and Synergistic Effect of SWCNTs-TiF3 on Hydrogen Uptake and Release from MgH2. Int. J. Hydrogen Energy 2014, 39, 14255–14261.
49. Amirkhiz, B.S.; Danaie, M.; Barnes, M.; Simard, B.; Mitlin, D. Hydrogen Sorption Cycling Kinetic Stability and Microstructure of Single-Walled Carbon Nanotube (SWCNT) Magnesium Hydride (MgH2) Nanocomposites. J. Phys. Chem. C 2010, 114, 3265–3275.
50. Verón, M.G.; Troiani, H.; Gennari, F.C. Synergetic Effect of Co and Carbon Nanotubes on MgH2 Sorption Properties. Carbon 2011, 49, 2413–2423.
51. Chuang, Y.-S.; Hwang, S.-J. Synthesis and Hydrogen Absorption/Desorption Properties of Mg–Nb2O5 -SWCNT/MWCNT Nanocomposite Prepared by Reactive Milling. J. Alloys Compd. 2016, 656, 835–842.

52. Gajdics, M.; Spassov, T.; Kis, V.K.; Schafler, E.; Révész, Á. Microstructural and Morphological Investigations on Mg-Nb2O5-CNT Nanocomposites Processed by High-Pressure Torsion for Hydrogen Storage Applications. Int. J. Hydrogen Energy 2020, 45, 7917–7928.
53. Révész, Á.; Spassov, T.; Kis, V.K.; Schafler, E.; Gajdics, M. The Influence of Preparation Conditions on the Hydrogen Sorption of Mg-Nb2O5-CNT Produced by Ball Milling and Subsequent High-Pressure Torsion. J. Nanosci. Nanotechnol. 2020, 20, 4587–4590.
54. Gajdics, M.; Spassov, T.; Kis, V.K.; Béke, F.; Novák, Z.; Schafler, E.; Révész, Á. Microstructural Investigation of Nanocrystalline Hydrogen-Storing Mg-Titanate Nanotube Composites Processed by High-Pressure Torsion. Energies 2020, 13, 563.